ACS chemical biology

Articles

pubs.acs.org/acschemicalbiology

^{13}C Tracer Reveals Phenolic Acids Biosynthesis in Hairy Root Cultures of *Salvia miltiorrhiza*

Peng Di,[†,#] Lei Zhang,[‡,#] Junfeng Chen,[†] Hexin Tan,[‡] Ying Xiao,[†] Xin Dong,[§] Xun Zhou,[†] and Wansheng Chen*[,†,∥]

[†]Department of Pharmacy, Changzheng Hospital, [‡]Department of Pharmacognosy, School of Pharmacy, [§]Department of Drug Analysis, School of Pharmacy, and [∥]Modern Research Center for Traditional Chinese Medicine, Second Military Medical University, Shanghai 200003, China

Supporting Information

ABSTRACT: Rosmarinic acid (RA) and lithospermic acid B (LAB) are two typical phenolic acids with significant bioactivities that may contribute to the therapeutic effects of *Salvia miltiorrhiza*. Precise knowledge of the biosynthetic pathway leading to RA and LAB is a necessary prerequisite to optimize the production of important phenolic compounds in *S. miltiorrhiza*. *In vivo* isotopic labeling experiments using [ring-^{13}C]-phenylalanine, combined with dynamic measurements of metabolite levels by UPLC/Q-TOF, were used to investigate the metabolic origin of phenolic acids in *S. miltiorrhiza*. These data indicate the *in vivo* phenolic biosynthetic pathway: two intermediates from the general phenylpropanoid pathway and the tyrosine-derived pathway, 4-coumaroyl-CoA and 3,4-dihydroxyphenyllactic acid (DHPL), are coupled by the ester-forming enzyme rosmarinic acid synthase (*Sm*RAS) to form 4-coumaroyl-3′,4′-dihydroxyphenyllactic acid (4C-DHPL). The 3-hydroxyl group is introduced late in the pathway by a cytochrome P450-dependent monooxygenase (*Sm*CYP98A14) to form RA. Subsequently, RA is transformed to a phenoxyl radical by oxidation, and two phenoxyl radicals unite spontaneously to form LAB. The results indicate aspects of the complexity of phenolic acid biosynthesis in *S. miltiorrhiza* and expand an understanding of phenylpropanoid-derived metabolic pathways. The candidate genes for the key enzymes that were revealed provide a substantial foundation for follow-up research on improving the production of important phenolic acids through metabolic engineering in the future.

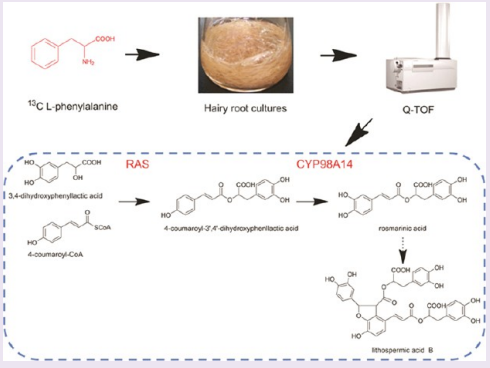

Plants have been estimated to synthesize a remarkably diverse array of over 100,000 low-molecular-mass natural products, also known as secondary metabolites, many of which have useful applications in the production of foods, industrial compounds, and pharmaceuticals.[1] An in-depth understanding of secondary metabolite biosynthetic pathways, along with the increasing number of cloned genes involved in biosynthesis, enables the exploration of metabolic engineering as a potentially effective approach to increase the yield of specific metabolites by enhancing rate-limiting steps or by blocking competitive pathways. Various pathways have been altered using genes encoding biosynthetic enzymes or genes encoding regulatory proteins in order to enhance pharmaceutically important compound production using this strategy in microbial systems.[2,3] However, a major constraint is the relatively poor characterization of plant secondary metabolic pathways at the level of the biosynthetic intermediates and enzymes. Feeding stable isotope labeled precursors accompanied by real time LC/GC−MS to analyze the labeling patterns is a powerful tool to investigate these pathways in plants. In recent years, some successful applications of this ^{13}C tracer method for investigation of *in vivo* biosynthetic pathways in petunia petal tissue[4] and *Datura innoxia* hairy root cultures[5] have been reported.

Salvia miltiorrhiza Bunge (Chinese name: Danshen) is a perennial herb of the Lamiaceae family. Its roots have been used for the treatment of cardiovascular diseases, blood circulation disturbance, inflammation, and angina pectoris for more than 2,000 years. The phenolic acids, including rosmarinic acid (RA) and lithospermic acid B (LAB), attracted interest in the past 20 years because of their notable pharmacological activities and the conventional use of the herb by decocting with water.[6] The composition and content of the phenolic acids are closely related to the quality of *Salvia*. In the process of large-scale cultivation, about 40% of the plant materials are unacceptable due to germplasm degradation, and this is a serious impediment to the clinical application of this plant. However, relatively little is known about phenolic acid biosynthesis in *S. miltiorrhiza*, and this has hampered the application of conventional molecular and genetic techniques to

Received: December 17, 2012
Accepted: April 24, 2013
Published: April 24, 2013

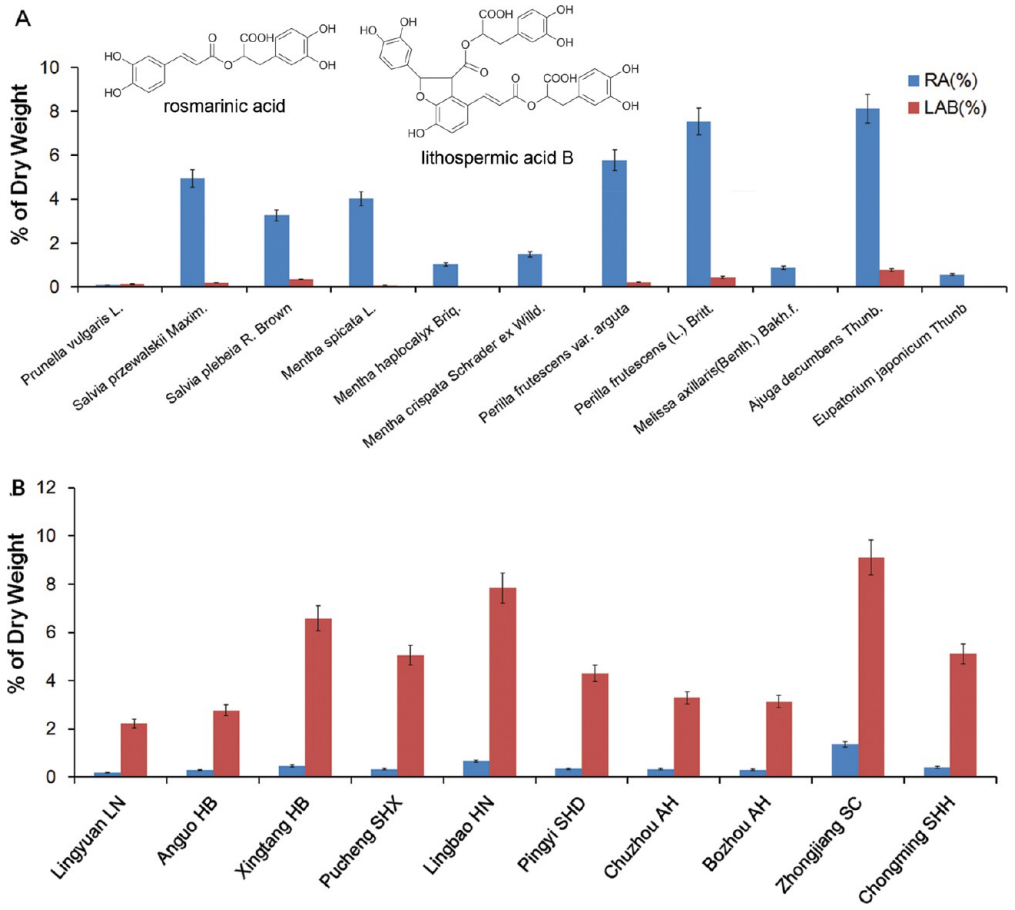

Figure 1. Accumulation pattern of rosmarinic acid (RA) and lithospermic acid B (LAB). (A) Accumulation pattern of RA and LAB in different Lamiaceae species. (B) Accumulation pattern of RA and LAB in *S. miltiorrhiza* from different habitats.

improve the quality and productivity of these metabolites using metabolic engineering.

Rosmarinic acid (RA) is an ester of caffeic acid and 3,4-dihydroxyphenyllactic acid. The biosynthetic pathway for RA had been thoroughly described at the molecular level in suspension cultures of *Coleus blumei* Benth.[7] The intermediary precursors, 4-coumaroyl-CoA, formed from L-phenylalanine and 4-hydroxyphenyllactate (pHPL), derived from L-tyrosine, are coupled in a transesterification reaction. Finally, this ester is hydroxylated by a cytochrome P450 monooxygenase at the C-3 and C-3′ in the aromatic nuclei to form RA.[8] The enzymes involved in this pathway have been isolated and characterized in suspension cultures of *Anchusa officinalis* L. (Boraginaceae) and *C. blumei* (Lamiaceae).[9,10] The cDNAs of phenylalanine ammonia-lyase (*Sm*PAL)[11] and cinnamic acid 4-hydroxylase (*Sm*C4H),[12] which are involved in the upstream metabolic processes of the general phenylpropanoid pathway, and tyrosine aminotransferase (*Sm*TAT),[13] 4-hydroxyphenylpylpyruvate reductase (*Sm*HPPR) (unpublished data), 4-hydroxyphenylpyruvate dioxygenase (*Sm*HPPD),[14] which are located in the tyrosine branch, have been successively cloned in our laboratory. Hydroxycinnamate:coenzyme A ligases (*Sm*4CLs) were cloned by Zhao et al.[15] Even though rosmarinic acid synthase (RAS), which links 4-coumaroyl-CoA and the aliphatic hydroxyl group of hydroxyphenyllactate,[16] and the subsequent cytochrome P450-dependent hydroxylases[8] are probably the most specific enzymes of the RA biosynthetic pathway, they have not yet been unraveled in *S. miltiorrhiza*. Due to the significant species-specificity of plant secondary metabolism, there is considerable interest in exploring the RA biosynthetic pathway in *S. miltiorrhiza*.

RA is the dominant phenolic acid present in species of the Lamiaceae (Figure 1A) except in *S. miltiorrhiza*, where the LAB content is consistently significantly higher than that of RA among various habitats (Figure 1B). This is also true in *S. miltiorrhiza* hairy root cultures, where the content of LAB was found to be much higher than that of RA.[17] Therefore, this unique accumulation pattern of phenolic metabolites (the ratio of RA/LAB) strongly suggests that an unknown biosynthetic pathway from RA to LAB is particularly active in *S. miltiorrhiza*. Although evidence that RA is a precursor leading to LAB synthesis and is presumed involved in a potential biosynthesis process from RA to LAB based on chemical structure analysis was provided by our laboratory,[18] the detailed biosynthetic process from RA to LAB remains unknown. In order to obtain enhanced knowledge regarding the biosynthesis of the phenolic compounds in *S. miltiorrhiza*, it is of great significance to elucidate the enzymatic steps downstream and to characterize the applicable enzymes.

In this report, the application of *in vivo* stable isotope labeling and dynamic measurements of metabolite levels in [ring-^{13}C]-phenylalanine fed *S. miltiorrhiza* hairy root cultures using UPLC/Q-TOF are described, in order to elucidate the biosynthetic pathway of the phenolic acids. The cloning and expression pattern of RAS and cytochrome P450 monooxygenase CYP98A14 and their involvement in the accumulation

dx.doi.org/10.1021/cb3006962 | *ACS Chem. Biol.* 2013, 8, 1537−1548

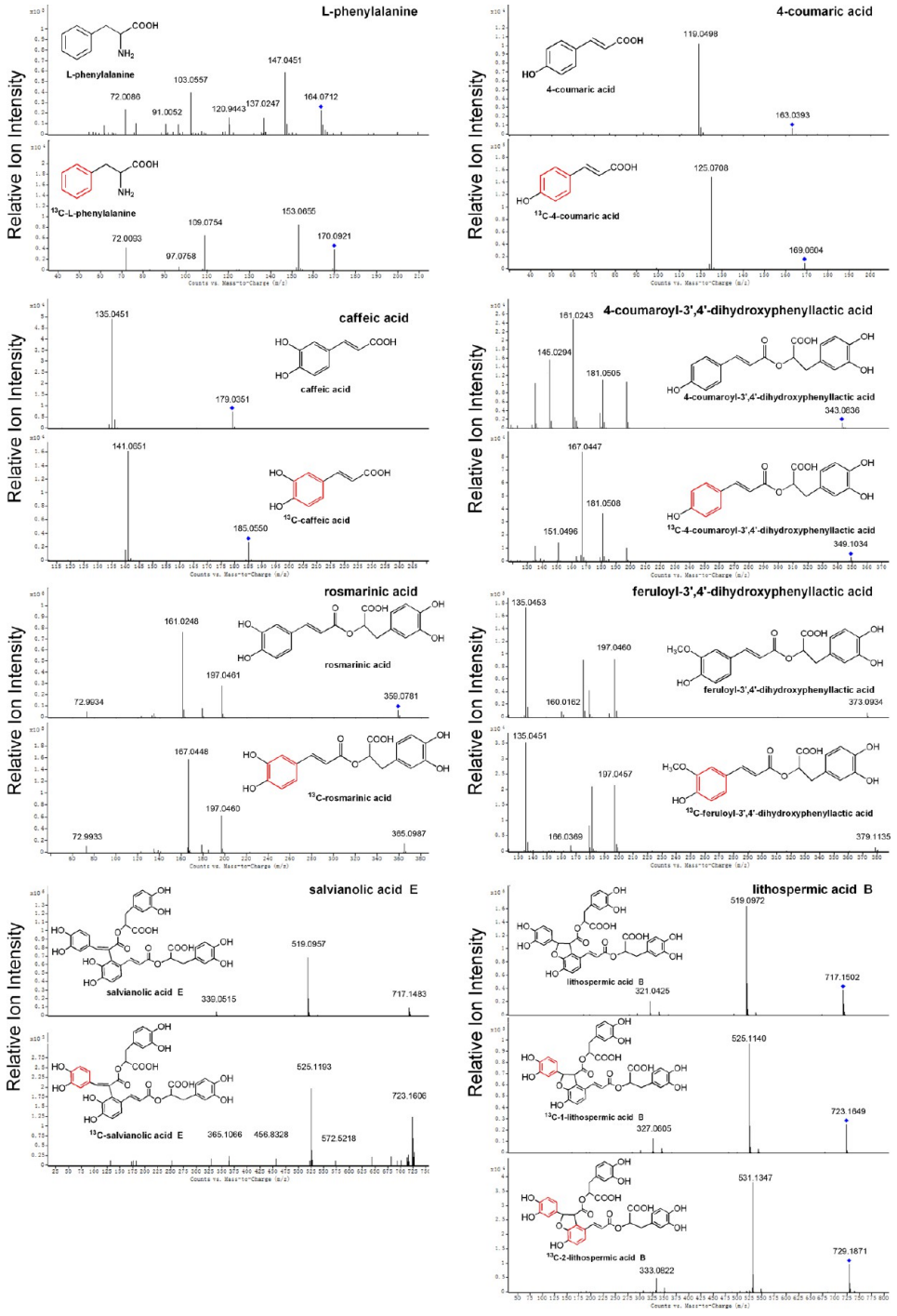

Figure 2. LC−MS/MS^n analysis of compounds identified involved in the phenolic acid biosynthesis pathway produced by *S. miltiorrhiza* hairy root culture fed with $^{13}C_6$-Phe. The panel for each presented compound contains the mass spectrum representing a combination of unlabeled and labeled compound extracted from the $^{13}C_6$-Phe-fed hairy root. All newly synthesized labeled phenolic acid compounds exhibit a mass shift of 6 atomic mass units (amu); LAB exhibited a shift of 12 amu based on the labeling of two aromatic rings.

of phenolic acids in the hairy root cultures of this plant are also presented. It is demonstrated that knowledge of secondary metabolism in partially species can be derived by using well-designed ^{13}C tracer experiments and integrating the labeling measurement data. This study describes the first ^{13}C tracer study for mapping the *in vivo* phenolic biosynthetic pathway in *S. miltiorrhiza*. This knowledge will assist in promoting the possibility of a gene-based metabolic engineering for the enhanced synthesis the active pharmaceutical compounds in *S. miltiorrhiza.*

RESULTS AND DISCUSSION

***In Vivo* Tracer Experiments.** The elucidation of the RA biosynthesis pathway in *C. blumei*[7] permitted the monitoring of its labeling pattern after supplying a labeled precursor in *S. miltiorrhiza*. In the labeling experiments, carbon-13 (^{13}C) ring-labeled Phe ($^{13}C_6$-Phe) was supplied to *S. miltiorrhiza* hairy

dx.doi.org/10.1021/cb3006962 | *ACS Chem. Biol.* 2013, 8, 1537−1548

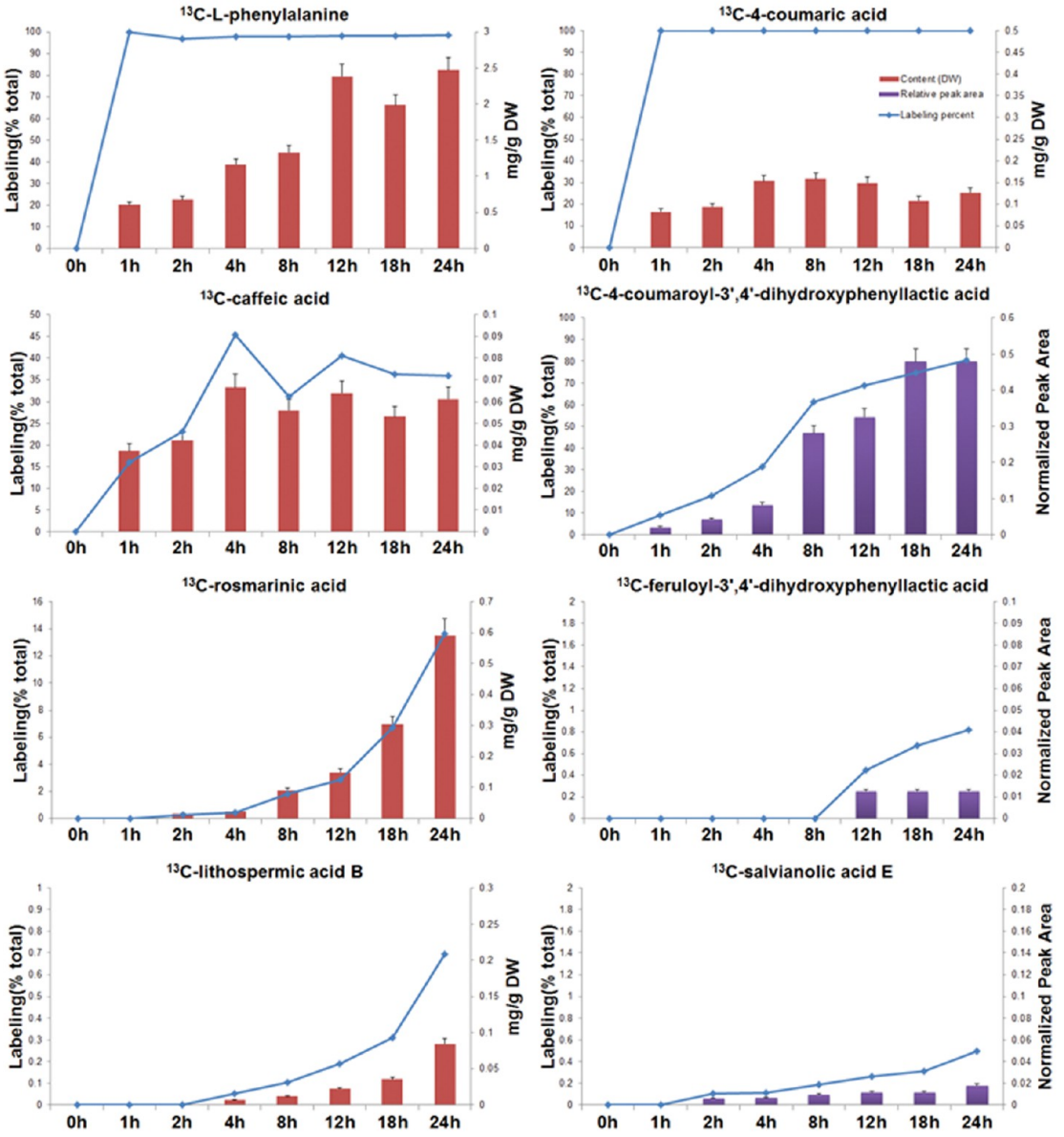

Figure 3. *In vivo* labeling kinetics of phenolic acid compounds during 24 h after feeding *S. miltiorrhiza* hairy root with $^{13}C_6$-Phe. The curves represent the percent of labeled compounds. The red bars represent the content of labeled compounds, and the violet bars represent the relative abundance of the labeled compounds. The relative abundance was calculated by dividing each peak area value by the internal standard peak area value.

root cultures, which can accumulate abundant phenolic acids *in vivo*.[19] Hairy roots were collected at 24, 48, 72, 96, and 144 h under dark conditions continuously fed with 1 mM $^{13}C_6$-Phe, then extracted with 30% methanol, and analyzed by liquid chromatography−mass spectrometry (UPLC/Q-TOF) to screen for the labeled endogenous metabolites. A total of 111 compounds were identified as the isotopomers synthesized from the supplied $^{13}C_6$-Phe (Supplementary Table S1). Among them, eight compounds, including L-phenylalanine, 4-coumaric acid, caffeic acid, 4-coumaroyl-3′,4′-dihydroxyphenyllactic acid (4C-DHPL), RA, feruloyl-3′,4′-hydroxyphenyllactic acid, salvianolic acid E (SAE), and LAB, were considered as the intermediates and end products involved in the phenolic acid pathway in *S. miltiorrhiza* (Figure 2).

In a time course experiment, hairy roots were exposed to $^{13}C_6$-phe (1 mM) up to 24 h. Concentrations and isotope abundances of ^{13}C-labeled metabolites in the hairy root cultures were followed over 24 h of culture. Isotope abundance was determined as $(^{13}C_6 \times 100)/(^{13}C_6 + {}^{12}C_6)$ (atom %). After extraction with 30% methanol, samples were analyzed by UPLC/Q-TOF-MS, and the experimentally obtained results are summarized in Figure 3. As a consequence, the ^{13}C label was detected in L-phenylalanine, 4-coumaric acid, caffeic acid, 4C-DHPL, RA, feruloyl-3′,4′-hydroxyphenyllactic acid, SAE, and LAB. $^{13}C_6$-Phe fed to the culture medium was efficiently taken up by *S. miltiorrhiza* hairy roots within 1 h. $^{13}C_6$-Phe was rapidly incorporated into 4-coumaric acid and caffeic acid, the single aromatic ring compounds, and the double aromatic ring compound 4C-DHPL within 1 h. It was then incorporated into RA and SAE at 2 h, and into LAB at 4 h. Finally, it incorporated into feruloyl-3′,4′-hydroxyphenyllactic acid after 12 h.

The content and normalized peak area represented the accumulation status of the labeled compounds during the feeding experiment. The highly accumulated compounds in this

dx.doi.org/10.1021/cb3006962 | *ACS Chem. Biol.* 2013, 8, 1537−1548

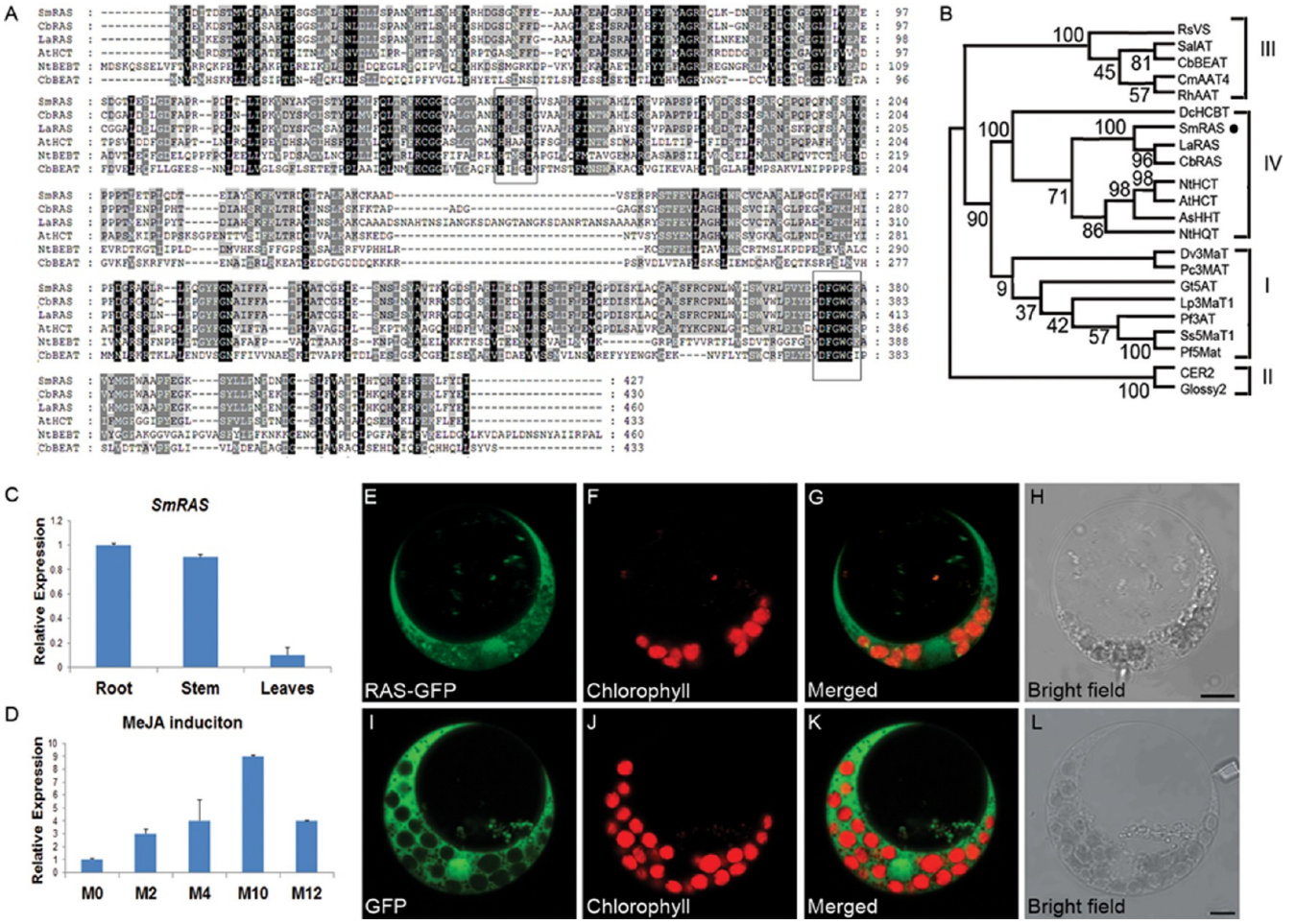

Figure 4. Characterization, expression, phylogenetic analysis, and subcellular localization of *SmRAS* protein. (A) Comparison of the predicted amino acid sequence of *Sm*RAS with related proteins. *S. miltiorrhiza* RAS sequence (*Sm*RAS, FJ906696) was aligned with RAS from *C. blumei* (*Cb*RAS, AM283092), RAS from *L. Angustifolia* (*La*RAS, AEA36976), HCT from *Arabidopsis* (*At*HCT, NP_199704), BEBT from *N. tabacum* (*Nt*BEBT, AAN09798) and BEAT, *C. breweri* (*Cb*BEAT, AAC18062) using Clustal X2. This alignment was shaded using GENEDOC. Identical and similar amino acids are shaded in black and gray, respectively. Boxes indicate the HxxxD and DFGWG motifs, respectively. (B) Phylogenetic tree of BAHD acyltransferases including RAS. The tree was constructed by neighbor-joining distance analysis by MEGA 5.05. Details concerning the proteins in the phylogenetic tree can be found in the Supporting Information. (C) Tissue specificity expression of *SmRAS*. (D) *SmRAS* expression under the induction of MeJA. (E–L) Analysis of *Sm*RAS subcellular localization. (E) A rice protoplast expressing RAS-GFP showing green fluorescent signals. (F) The same protoplast cell of panel E showing the chlorophyll autofluorescence signal in the plastids. (G) The merged signal of panels E and F. (H) Bright-field image of panel E. (I) A rice protoplast expressing GFP showing green fluorescent signals. (J) The same protoplast cell of panel I showing the chlorophyll autofluorescence signal in the plastids. (K) The merged signal of panels I and J. (L) Bright-field image of panel I. Bars = 5 μm.

pathway were 4-coumaric acid, caffeic acid, 4-coumaroyl-3′,4′-dihydroxyphenyllactic acid, RA, and LAB. Other metabolites, such as feruloyl-3′,4′-dihydroxyphenyllactic acid and SAE, accumulated at a low level. The isotope labeling curves, and the content variations, of the eight compounds demonstrated the *de novo* biosynthesis of these compounds from exogenous phenylalanine. The $^{13}C_6$-Phe incorporated into RA and SAE at 2 h, and incorporated into LAB at 4h. The pool of RA was more heavily labeled than the LAB pool, and $^{13}C_6$-Phe was incorporated into RA earlier than LAB, suggesting that RA is the precursor for LAB in *S. miltiorrhiza.* LAB with two aromatic rings labeled with $^{13}C_6$ was also detected (Figure 2), which was probably derived through the coupling of two molecules of labeled $^{13}C_6$-RA.

Examination of the aromatization and substitution patterns of RA, SAE, and LAB, combined with the labeling curves, led to the conclusion that LAB was directly derived from RA, and that the intermediate might be SAE. A mechanism for the synthesis of SAE and LAB from RA could be proposed. Oxidation of the 4-OH and 3-OH of the RA moieties results in formation of the phenoxyl radicals or semiquinones "A" and "B", respectively, catalyzed by an unknown oxidase. The coupling of one radical "A" and one radical "B", followed by tautomeric rearrangement and intramolecular nucleophilic attack, would afford the intermediate quinone "C". Subsequently, the quinone "C" would be converted to LAB *via* SAE or directly converted to LAB by spontaneous reaction.[20−22]

Combined with the isotope labeling curves and the accumulation states of these compounds, it was possible to project a phenolic acid biosynthetic pathway in *S. miltiorrhiza.* The pathway starts from the general phenylpropanoid pathway and the tyrosine-derived pathway. Ester formation by *Sm*RAS to form 4C-DHPL and then 3-hydroxylation by *Sm*CYP98A14 afford RA. Subsequently, two molecules RA are oxidatively

dx.doi.org/10.1021/cb3006962 | *ACS Chem. Biol.* 2013, 8, 1537−1548

coupled to form SAE and LAB by spontaneous reaction. Caffeic acid and feruloyl-3′,4′-hydroxyphenyllactic were presumed to be bypass products involved in this pathway, respectively. Compared with the RA biosynthesis pathway in *C. blumei*, 4C-DHPL was considered as the main intermediate for RA biosynthesis in *S. miltiorrhiza*, and 3′,4′-dihydroxyphenyllactic acid (DHPL) was involved in this pathway as a principal intermediate.

Isolation and Characterization of *SmRAS*. *Sm*RAS cDNA (accession no. FJ906696) contained a 1284-bp ORF, encoding a predicted 426-amino-acid polypeptide. The sequence contains all the characteristic elements of the BAHD enzymes,[23] two conserved site HXXXD and DFGWG domains, signature of BAHD superfamily members, were found by multiple sequence alignment (Figure 4A). The protein−protein BLAST analysis showed that *Sm*RAS was most similar (identity 81%, similarity 87%) to a hydroxycinnamoyl transferase from *C. blumei* (*Cb*RAS, GenBank accession no. CAK55166).

To determine the relationship of *Sm*RAS to other BAHD acyltransferases, a nonrooted phylogenetic tree was constructed from 22 BAHD acyltransferases with known sequence and function along with *S. miltiorrhiza* RAS (Figure 4B). The tree clearly showed four classes of BAHD acyltransferases with their respective subgroups.[23] All of the sequences were classified into four clades, as previous described.[23] *Sm*RAS belongs to a clade of class IV, which comprises the enzymes that transfer aromatic acyl moieties, and was grouped with *Cb*RAS and *La*RAS. *Cb*RAS preferentially accepts 4-coumaroyl-CoA and caffeoyl-CoA, transferring the aromatic acyl groups to pHPL and DHPL.[24] *La*RAS exhibits substrate promiscuity and catalyzes the formation of tyramine derivatives and the formation of (hydroxy) cinnamoyl esters.[25] Both of these two enzymes catalyze the formation of 4-coumaroyl-4′-hydroxyphenyllactic acid (4C-pHPL), the precursor of RA.

Analysis of the *SmRAS* gene transcription level in the roots, stems, and leaves by RT-qPCR revealed that *SmRAS* was expressed predominantly in roots and stems (Figure 4C). Roots were previously shown to be the main organ for the synthesis and accumulation of RA and related phenolic compounds in *S. miltiorrhiza*. The transcription level of *SmRAS* was sensitive to methyl jasmonate (MeJA). After treatment with 0.1 mM MeJA, the *SmRAS* transcription level increased sharply and peaked at 8 h with an increase about 9-fold (Figure 4D).

Like most BAHD members,[26] *Sm*RAS has no transit peptides or other sequences that will lead to localization in organelles or to secretion. Currently, most identified members of the BAHD family are thought to be localized to the cytosol,[23] while *Mt*MaT1 is nucleocytoplasm-localized, and the C-terminal DFGWG motif is necessary for its localization.[27] To experimentally verify the subcellular localization of *Sm*RAS, the full length *Sm*RAS coding sequence was fused in-frame to the N-terminus of enhanced GFP. The constructs *Sm*RAS-GFP and GFP alone were introduced into protoplasts isolated from etiolated rice stems. As shown in Figure 4E−H, the fluorescence of the *Sm*RAS−GFP fusion was distributed in both the cytoplasm and nuclei, as was GFP itself (Figure 4I−L), and this result was confirmed by tobacco leaves injection experiment. These observations support the idea that *Sm*RAS is clearly localized not only in the cytoplasm but also in nuclei.

SmRAS antisense transgenic *S. miltiorrhiza* hairy root lines were established to investigate the influence of RAS interruption for phenolic acid biosynthesis. *SmRAS* was successfully suppressed through genetic manipulation. Its transcription level was decreased in each transgenic line with the average being 45% of control. Especially in the R5 line, the transcript level decreased to about 24% of the CK line (Figure 5A). Meanwhile, the transcript profile analysis of the R5 line

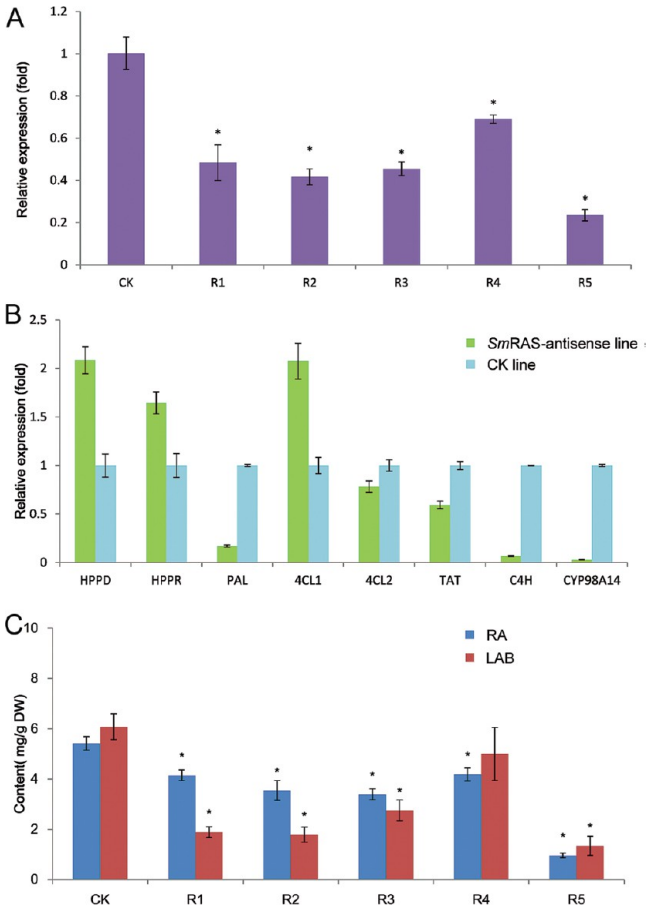

Figure 5. Analysis of gene expression and pheolic acid accumulation in *SmRAS*-antisesnse hairy root lines. (A) Quantification of the transcriptions of *SmRAS* in different transgenic lines. (B) Quantification of the transcription levels of RA biosynthetic genes in *SmRAS*-antisense hairy root line R5. (C) RA and LAB accumulation in *SmRAS*-anisense hairy root lines. Asterisk indicates that difference is significant at $p < 0.05$ compared with CK. CK: vector control; R1-R5: RAS-antisense lines.

showed a depression of *SmRAS* and also variably affected the transcription level of several other RA biosynthetic genes. *PAL1* and *C4H*, the genes encoding the enzymes catalyzing the first two steps of the phenylpropanoid pathway, were down-regulated dramatically. Two *4CL* genes, *4CL1* and *4CL2*, were regulated in different manners. The gene *4CL2* was down-regulated slightly; however, in contrast, *4CL1* was up-regulated 2-fold that of the control. *TAT*, which catalyzed the first steps on the tyrosine branch, was down-regulated slightly, whereas the other two genes, *HPPD* and *HPPR*, were up-regulated about 2- and 1.5-fold compared with the control, respectively. The transcription level of *CYP98A14* was dramatically decreased (Figure 5B). The content of RA and LAB in transgenic hairy root lines was determined by triple-quadrupole mass spectrometry in order to investigate the correlation between *SmRAS* and the accumulation of phenolic acids. Compared with the CK lines (RA: 5.41 mg g^{-1} DW, LAB: 6.07

dx.doi.org/10.1021/cb3006962 | *ACS Chem. Biol.* 2013, 8, 1537−1548

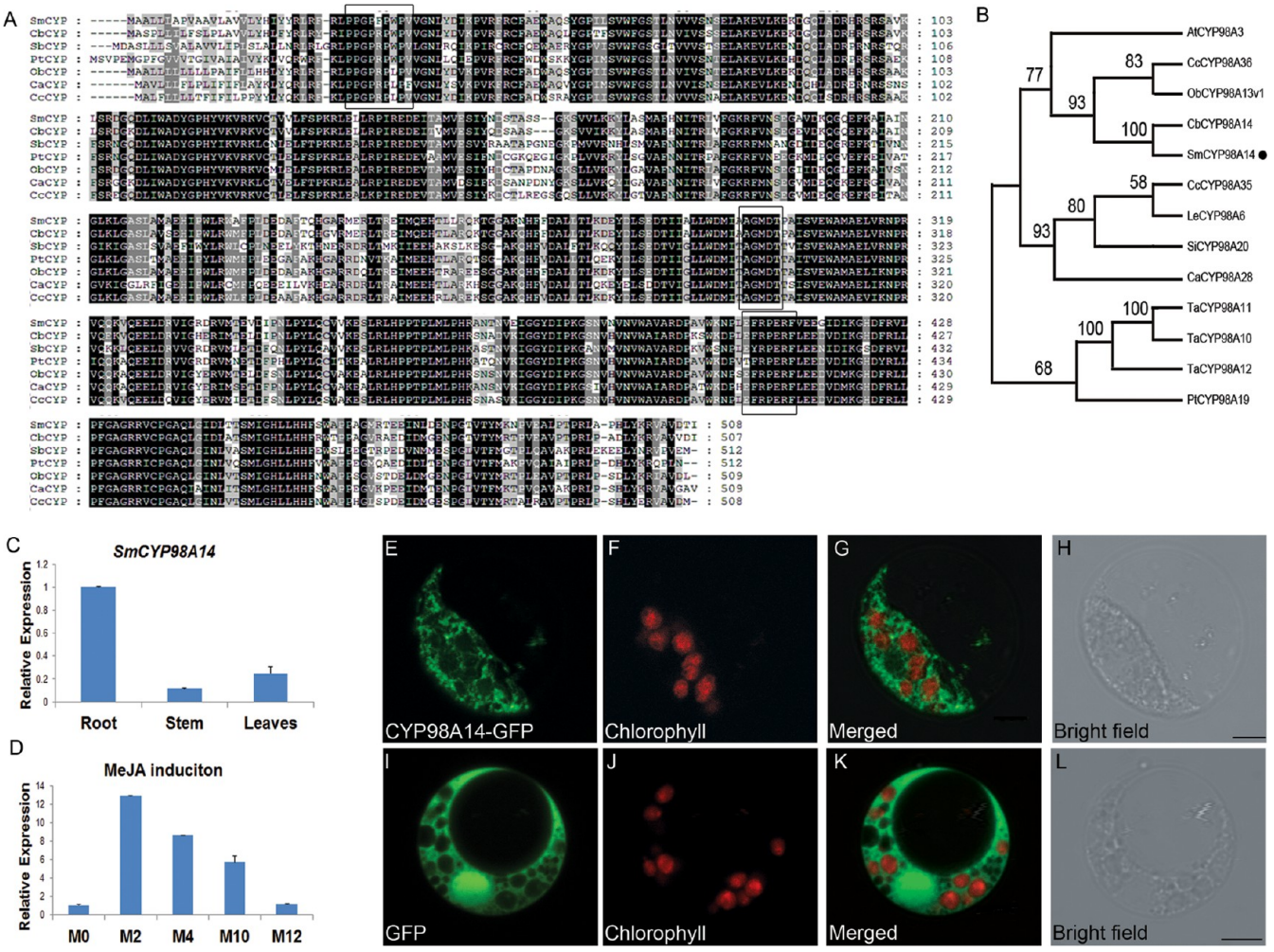

Figure 6. Characterization, expression, phylogenetic analysis, and subcellular localization of *SmCYP98A14* protein. (A) Comparison of the predicted amino acid sequence of *Sm*CYP98A14 with related proteins. *S. miltiorrhiza* CYP98A14 sequence (*Sm*CYP98A14, HQ316179) was aligned with CYP98A14 from *C. blumei* (*Cb*CYP98A14, AJ427452), CYP98A1 from *S. bicolor* (*Sb*CYP98A1, AF029856), *p*-coumarate 3-hydroxylase from *P. taeda* (*Pt*CYP, AY064170), *p*-coumaroylshikimate 3′-hydroxylase from *O. basilicum* (*Ob*CYP, AY082612), *p*-coumaroyl 3′-hydroxylase from *C. canephora* (*Cc*CYP, DQ269127), and hydroxylase-like cytochrome P450 from *C. acuminata* (*Ca*CYP, AY466856) using Clustal X. This alignment was shaded using GENEDOC. Identical and similar amino acids are shaded in black and gray, respectively. Boxes indicate the proline-rich region, the O_2 binding site, the PERF-motif locationed, and the heme binding cysteine motif, respectively. (B) Phylogenetic tree of CYP98As, including CYP98A14. The tree was constructed by neighbor-joining distance analysis by MEGA 5.05. Details about the proteins in the phylogenetic tree can be found in the Supporting Information. (C) Tissue specificity expression of *SmCYP98A14*. (D) *SmCYP98A14* expression under the induction of MeJA. (E–L) Analysis of *SmCYP98A14* subcellular localization. (E) A rice protoplast expressing CYP98A14-GFP showing green fluorescent signals. (F) The same protoplast cell of panel E showing the chlorophyll autofluorescence signal in the plastids. (G) The merged signal of panels E and F. (H) Bright-field image of panel E. (I) A rice protoplast expressing GFP showing green fluorescent signals. (J) The same protoplast cell of panel I showing the chlorophyll autofluorescence signal in the plastids. (K) The merged signal of panels I and J. (L) Bright-field image of panel I. Bars = 5 μm.

mg g^{-1} DW), the accumulation of RA and LAB was obviously decreased in transgenic lines to 59% and 42% of control on average (Figure 5C). The maximum decrease was detected in the line R5 with 0.95 mg g^{-1} DW of RA and 1.34 mg g^{-1} DW of LAB. This result closely correlated with the transcription pattern of *SmRAS* in the antisense lines.

Isolation and Characterization of *SmCYP98A14*. *Sm*CYP98A14 cDNA encodes an ORF of 1524 nucleotides, corresponding to a 508-amino-acid protein with a calculated molecular mass of 57 kDa and a p*I* of 8.23 (GenBank accession no. HQ316179). The protein encoded by this cDNA has 87% and 77% amino acid identity to the CYP from *C. blumei*[8] and *O. basilicum*,[28] respectively. The CYP98A14 amino acid sequence revealed elements generally found in the CYP98 family, for example, the proline-rich region, the O_2 binding site,[29] the PERF motif,[30] and the heme binding, cysteine motif[31] (Figure 6A).

Fifteen CYP98A proteins, which have been characterized by their enzyme activities as 4-hydroxycinnamoyl shikimate/quinate 3-hydroxylases or 4-coumarate 3-hydroxylases, were collected for phylogenetic analysis (Figure 6B). *Sm*CYP98A14 was grouped with CYP98A14 from *C. blumei*[8] and CYP98A13v1 from *O. basilicum*.[28] *C. blumei* CYP98A14 was reported to only accept RA-like esters,[8] and CYP98A13s most actively catalyzed the 3-hydroxylation of 4-coumaroyl shikimate/quinate, also with low efficiency for the hydroxylation of hydroxyphenyllactate esters.[28]

dx.doi.org/10.1021/cb3006962 | *ACS Chem. Biol.* 2013, 8, 1537–1548

SmCYP98A14 was expressed significantly high in roots, but weakly in stems and leaves (Figure 6C). *SmCYP98A14* was sensitive to MeJA, but with a different variation pattern compared tothat of *SmRAS*. After treatment with 0.1 mM MeJA, the expression level of *SmCYP98A14* increased sharply and peaked at 2 h with an increase of about 13-fold and then decreased to the initial level after 12 h (Figure 6D).

Cytochrome P450 enzymes are usually anchored via their N terminus on the cytoplasmic surface of the endoplasmic reticulum (ER) with the main protein fold protruding on the surface of the membrane.[32,33] As a member of the P450 family, *Sm*CYP98A14 has a transmembrane domain (amino acids 2–21), as detected by the TMHMM v2.0 program, and was predicted to be probably localized to ER by PSORT (http://psort.nibb.ac.jp/form.html). To experimentally verify the subcellular localization of *Sm*CYP98A14, we introduced *Sm*CYP98A14-GFP fusion and the GFP alone control, driven by the CaMV35S promoter, into protoplasts isolated from etiolated rice stems. As expected, *Sm*CYP98A14-GFP behaved as typical endoplasmic reticulum proteins (Figure 6E–H), whereas GFP were evenly distributed in the cytoplasm and the nucleus (Figure 6I–L). Therefore, the hydroxylation step catalyzed by *Sm*CYP98A14 is taking place in ER.

SmCYP98A14 antisense transgenic *S. miltiorrhiza* hairy root lines were established to investigate the effect of *SmCYP98A14* interruption on phenolic acid biosynthesis. In comparison with the CK line, expression of *SmCYP98A14* was decreased in each of the *CYP98A14*-antisense transgenic lines with an average of 40% of control line. Especially in the C4 line, the expression was decreased to 22% of the control line (Figure 7A). The transcription level of the genes involved in the pathway was also changed, with a pattern similar to that of the *SmRAS*-antisense lines. The genes *PAL1*, *C4H*, and *4CL2* were all down-regulated, while *4CL1* was increased about 2-fold. *TAT* showed a slight decrease, whereas *HPPR* and *HPPD* were up-regulated, and the *RAS* was suppressed slightly (Figure 7B).

The contents of RA and LAB in the *CYP98A14*-antisense transgenic lines were decreased to 44% and 81% of control on average compared with the CK line (12.25 mg g^{-1} DW of RA, 9.73 mg g^{-1} DW of LAB) (Figure 7C). The largest decrease in levels of RA was observed in the C4 line (3.59 mg g^{-1} DW of RA), a decrease to 28% that of the CK line. However, the changes of LAB concentration were more moderate with only mild effects.

Discussion. The initial steps for RA biosynthesis in *S. miltiorrhiza* were in accordance with those in *C. blumei*,[7] which belongs to the general phenylpropanoid pathway and tyrosine-derived pathway. In the $^{13}C_6$-Phe feeding experiment, $^{13}C_6$-4C-pHPL and $^{13}C_6$-Caf-pHPL were not detected, whereas $^{13}C_6$-4C-DHPL was detected at 2 h. In *C. blumei*, 4C-pHPL was considered as the precursor for 4C-DHPL and Caf-pHPL. However, the absence of 4C-pHPL and Caf-pHPL in *S. miltiorhiza* suggested that 4C-DHPL might be directly formed by *Sm*RAS rather than by 3-hydroxylation from 4C-pHPL. The substrates for the direct formation 4C-DHPL might be 4-coumaroyl-CoA and DHPL. This hypothesis was also supported by the feeding experiment (Supplementary Figure S1). A recent report concerning RAS substrate specificities in *C. blumei*, which showed the apparent K_m values of *Cb*RAS for DHPL (1.8 μM) and pHPL (9.2 μM) are different from the former results, which had suggested pHPL is the preferred substrate for RAS, also supported the present hypothesis.[16]

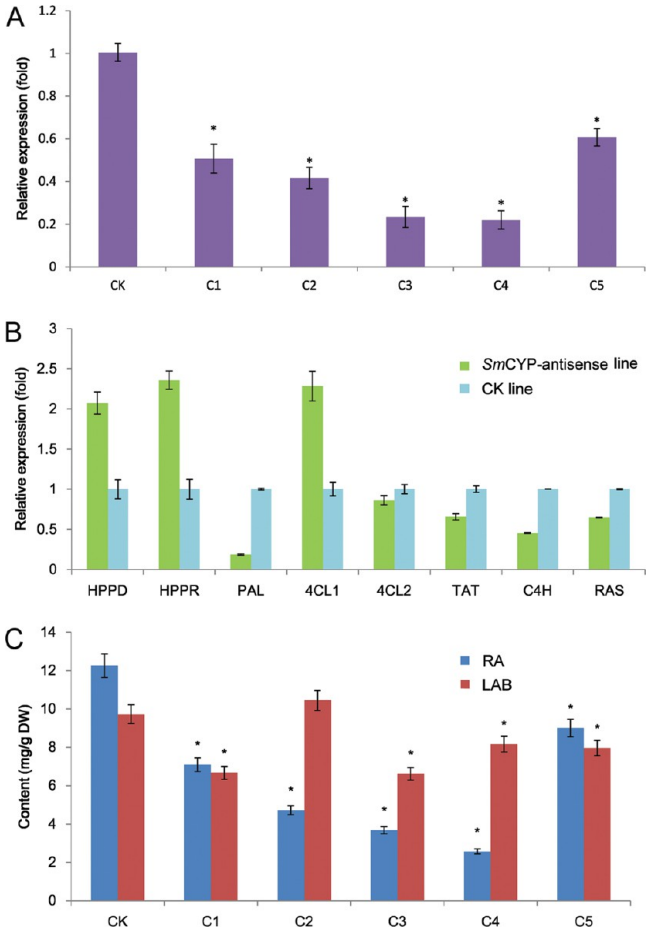

Figure 7. Analysis of gene expression and phenolic acid accumulation in *SmCYP98A14*-antisesnse hairy root lines. (A) Quantification of the transcription levels of *SmCYP98A14* in different transgenic lines. (B) Quantification of the transcription level of RA biosynthetic genes in the *SmCYP98A14*-antisense hairy root line C4. (C) RA and LAB accumulation in *SmCYP98A14*-anisense hairy root lines. Error bars show the standard deviations of independent lines. Asterisk indicates that difference is significant at $p < 0.05$ compared with CK. CK: vector control; C1–C5: SmCYP98A14-antisense lines.

The last two steps in RA biosynthesis are 3-/3′-hydroxylation and are catalyzed by CYP98A14 in *C. blumei*.[8] Only one substrate, 4C-DHPL, for CYP98A14 was detected in feeding experiments. This result implies that the 3-hydroxylation of 4C-pHPL and the 3′-hydroxylation of Caf-pHPL might not be occurring for RA biosynthesis in *S. miltiorrhiza* due to the absence of these substrates. Content determination of the extracts obtained from lavender flowers showed that only RA (2 mg g^{-1}) and its biogenetic precursor 4C-DHPL (0.15 mg g^{-1}) could be found; other potential products of RAS catalysis could not be detected.[25] This result is in accordance with the present observations that 4C-DHPL is the only ester intermediate for RA biosynthesis in *S. miltiorrhiza*.

The specific enzymes of the RA biosynthetic pathway were RAS and cytochrome P450 monooxygenase, which have been characterized in *C. blumei* and *Lithospermum erythrorhizon*.[8,24,34] However, these two enzymes have not yet been revealed in *S. miltiorrhiza*. Using a functional genomic approach, the cDNAs of *Sm*RAS and *Sm*CYP98A14 were isolated. RAS is a member of the BAHD acyltransferase family, which was reported to be highly expressed in stem of poplar and *Arabidopsis*.[26] The high

dx.doi.org/10.1021/cb3006962 | *ACS Chem. Biol.* 2013, 8, 1537–1548

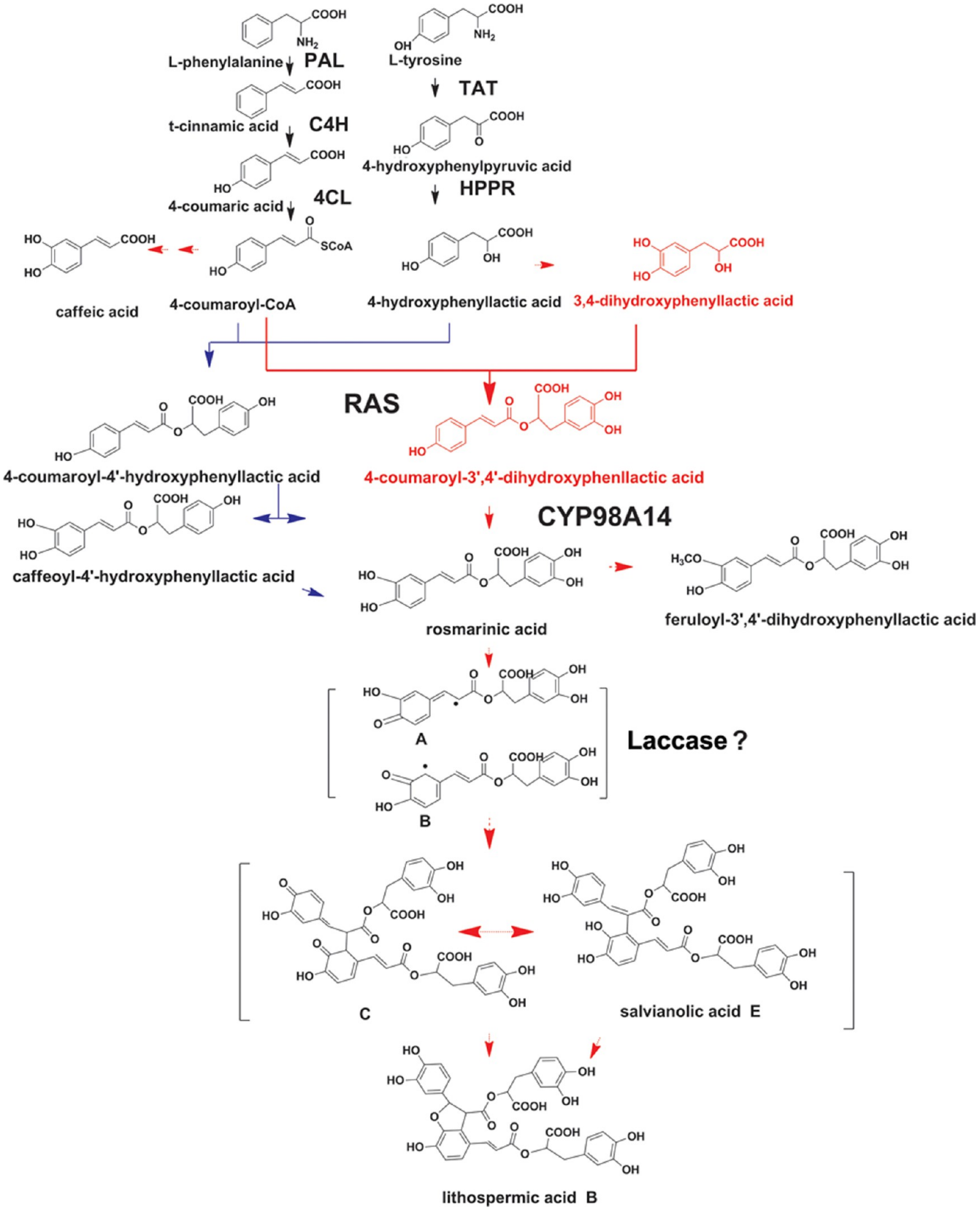

Figure 8. Proposed phenolic acid biosynthesis pathway in *S. miltiorrhiza*, which was drawn according to isotope tracer experiment results (denoted in red) and the rosmarinic acid biosynthesis pathway in *C. blumei*, which was previously reported by Petersen et al.[7] (denoted in blue). The solid line represents the verified biosynthesis process, whereas the dotted line represents the proposed biosynthetic process, which has not yet been verified by the identification of specific enzyme-mediated catalytic reactions.

dx.doi.org/10.1021/cb3006962 | *ACS Chem. Biol.* 2013, 8, 1537–1548

expression level of *SmRAS* in roots and stems indicated a potential role in the formation of phenolic acids. The expression patterns of *SmCYP98A14* were somewhat different compared with those of most CYP98A P450 subfamily members, which are highly expressed in stem and vascular bundles.[35] *SmCYP98A14* demonstrated strong expression in roots, but weak expression in stems and leaves. This result indicated that *SmCYP98A14* is specifically participating in the RA biosynthesis in roots, which was considered as the main organ for the synthesis and accumulation of phenolic compounds.

SmRAS was induced significantly by MeJA like the other BAHD family genes such as *MtMAT1*, *MtMAT2* in *Medicago truncatula*,[27] and *AtESP1* in *Arabidopsis*.[36] *CYP98A14* responded to MeJA induction quickly, peaking at 2 h with 13-fold increase. This was in accordance with the study in *L. erythrorhizon* cell suspension cultures that the expression of *CYP98A6* was massively stimulated after MeJA treatment.[34]

Antisense successfully suppressed *Sm*RAS and *Sm*CYP98A14 expression, followed with decreased RA and LAB accumulation in hairy root lines. These results provided solid *in vivo* proof that the two genes were involved in RA and LAB biosynthesis pathway.

Our previous research presumed that the biosynthetic route of LAB was as follows: RA and caffeic acid were catalyzed by an enzyme to synthesize an intermediate lithospermic acid (LA), and then LA reacted with DHPL to synthesize LAB through a spontaneous esterification process.[18] However, in this ^{13}C tracer experiment, the predicted intermediate, LA, was not detected, but rather SAE was observed to be the proposed intermediate for LAB. The dimerization process of hydroxystilbenes, which have similar aromatic rings as RA, has been well studied.[21] On the basis of the present results, it is hypothesized that a similar reaction mechanism might be operational in *S. miltiorrhiza*. Reports concerning the oxidative dimerization of hydroxystilbenes showed that this reaction was catalyzed by a basic oxidase, a laccase, in different plant species.[37,38] Here it is proposed that laccase was the potential enzyme that involved in the synthetic process between RA and LAB (Supplementary Figure S2). Thus, the gene encoding laccase (*Sm*LAC) was first isolated from *S. miltiorrhiza*, and the *Sm*LAC protein was successfully expressed in *E. coli* (Supplementary Figure S3). Subsequently, feeding experiments were conducted to examine the enzyme activity: *Sm*LAC successfully oxidized 2,2′-azinobis(3-ethylbenzthiazoline-6-sulfonate) (ABTS) to afford a green color after incubation, and meanwhile the RA concentration was also found to dramatically decrease, although the catalytic product was not observed (Supplementary Figure S4). These results demonstrated the important role of *Sm*LAC in catalyzing RA *in vitro*. However, this remains to be investigated in further studies, including as *in vivo* experiment.

In conclusion, the biosynthesis of phenolic acids in *S. miltiorrhiza* starts with L-phenylalanine and L-tyrosine, which are separately transformed to the intermediates 4-coumaroyl-CoA and DHPL. The transformation of L-phenylalanine is catalyzed by the enzymes of the general phenylpropanoid pathway, PAL, C4H, and 4CLs. Tyrosine is transformed by TAT to 4′-hydroxyphenylpyruvic acid (pHPP), which is then reduced to pHPL by HPPR, and then the 3′-hydroxyl group is introduced by an unknown cytochrome P450-dependent monooxygenase to form DHPL. The two intermediates are coupled by ester formation, and the released 4C-DHPL is catalyzed by RAS. The 3′-hydroxyl group is finally introduced by CYP98A14 to afford RA. The subsequent steps are proposed to be catalyzed by laccase, which could oxidize RA to the phenoxyl radicals "A" and "B". The coupling of one radical "A" and one radical "B", followed by tautomeric rearrangement and intramolecular nucleophilic attack yields the intermediate quinone "C". Subsequently, the quinone "C" is converted to LAB by way of SAE or may be directly converted to LAB by spontaneous reaction. Additionally, caffeic acid and feruloyl-3′,4′-dihydroxyphenyllactic acid are involved in this pathway as bypass products (Figure 8).

The current study expands the knowledge of phenylpropanoid derived metabolism and explains the *in vivo* phenolic acid biosynthetic process in *S. miltiorrhiza*. This work also sheds light on how to effectively elucidate the pathways of secondary metabolite biosynthesis for further genetic engineering or for the quality control of medicinal plants.

METHODS

Plant Material, Chemicals, and Radiochemicals. Details on the plant material, the chemicals, and the labeled chemicals can be found in the Supporting Information.

Labeling Experiments, Screening, and Identification of Labeled Compounds. The stable isotope labeling method is described in the Supporting Information. Screening and the identification of the labeled compounds using UPLC/Q-TOF-MS follows the methods described in the Supporting Information.

LC−MS/MS Analysis. The content of RA and LAB from the Lamiaceae plants, namely, *S. miltiorrhiza* from different habitats and *S. miltiorrhiza* transgenic hairy root cultures, were analyzed by LC−MS/MS according to the methods described in the Supporting Information.

Gene Clone, Subcellular Localization, and Transgenic Analysis. The information about the gene cloning and phylogenetic analysis of *SmRAS* and *SmCYP98A14* can be found in the Supporting Information. The details regarding the antisense vector construction and plant transformation can be found in the Supporting Information. Subcellular localization analysis followed the method described in the Supporting Information.

Statistical Analysis. Statistical analysis was performed with SPSS 13.0 software. Analysis of variance (ANOVA) was followed by Tukey's pairwise comparison tests, at a level of $p < 0.05$, to determine significant differences between means.

ASSOCIATED CONTENT

Supporting Information

This material is available free of charge via the Internet at http://pubs.acs.org.

AUTHOR INFORMATION

Corresponding Author

*E-mail: chenwanshengsmmu@yahoo.com.cn.

Author Contributions

#These authors contributed equally to this work.

Notes

The authors declare no competing financial interest.

ACKNOWLEDGMENTS

We thank F. Negre (Department of Plant Sciences, UC Davis) for her helpful discussions. This work was financially supported by the National Natural Science Foundation of China (31100221 and 31160059).

REFERENCES

(1) Dixon, R. A. (2001) Natural products and plant disease resistance. *Nature 411*, 843−847.

(2) Zhang, L., Ding, R., Chai, Y., Bonfill, M., Moyano, E., Oksman-Caldentey, K.-M., Xu, T., Pi, Y., Wang, Z., Zhang, H., Kai, G., Liao, Z., Sun, X., and Tang, K. (2004) Engineering tropane biosynthetic pathway in *Hyoscyamus niger* hairy root cultures. *Proc. Natl. Acad. Sci. U.S.A. 101*, 6786−6791.

(3) Xiao, Y., Zhang, L., Gao, S., Saechao, S., Di, P., Chen, J., and Chen, W. (2011) The c4h, tat, hppr and hppd genes prompted engineering of rosmarinic acid biosynthetic pathway in *Salvia miltiorrhiza* hairy root cultures. *PloS One 6*, e29713.

(4) Boatright, J., Negre, F., Chen, X., Kish, C. M., Wood, B., Peel, G., Orlova, I., Gang, D., Rhodes, D., and Dudareva, N. (2004) Understanding in vivo benzenoid metabolism in *petunia petal* tissue. *Plant Physiol. 135*, 1993−2011.

(5) Houssam, M., Balkhi, A., Schiltz, S., Lesur, D., Lanoue, A., Wadouachi, A., and Boitel-conti, M. (2012) Phytochemistry Norlittorine and norhyoscyamine identified as products of littorine and hyoscyamine metabolism by ^{13} C-labeling in *Datura innoxia* hairy roots. *Phytochemistry 74*, 105−114.

(6) Ma, L., Zhang, X., Guo, H., and Gan, Y. (2006) Determination of four water-soluble compounds in *Salvia miltiorrhiza* Bunge by high-performance liquid chromatography with a coulometric electrode array system. *J. Chromatogr., B: Anal. Technol. Biomed. Life Sci. 833*, 260−263.

(7) Petersen, M., Abdullah, Y., Benner, J., Eberle, D., Gehlen, K., Hücherig, S., Janiak, V., Kim, K. H., Sander, M., Weitzel, C., and Wolters, S. (2009) Evolution of rosmarinic acid biosynthesis. *Phytochemistry 70*, 1663−1679.

(8) Eberle, D., Ullmann, P., Werck-Reichhart, D., and Petersen, M. (2009) cDNA cloning and functional characterisation of CYP98A14 and NADPH:cytochrome P450 reductase from *Coleus blumei* involved in rosmarinic acid biosynthesis. *Plant Mol. Biol. 69*, 239−253.

(9) Petersen, M. (2003) Cinnamic acid 4-hydroxylase from cell cultures of the hornwort Anthoceros agrestis. *Planta 217*, 96−101.

(10) Petersen, M. (2007) Current status of metabolic phytochemistry. *Phytochemistry 68*, 2847−2860.

(11) Hu, Y., Zhang, L., Di, P., and Chen, W. (2009) Cloning and induction of phenylalanine ammonia-lyase gene from *Salvia miltiorrhiza* and its effect on hydrophilic phenolic acids levels. *Chin. J. Nat. Med. 7*, 449−457.

(12) Huang, B., Duan, Y., Yi, B., Sun, L., Lu, B., Yu, X., Sun, H., Zhang, H., and Chen, W. (2008) Characterization and expression profiling of cinnamate 4-hydroxylase gene from *Salvia miltiorrhiza* in rosmarinic acid biosynthesis pathway. *Russ. J. Plant Physiol. 55*, 390−399.

(13) Huang, B., Yi, B., Duan, Y., Sun, L., Yu, X., Guo, J., and Chen, W. (2008) Characterization and expression profiling of tyrosine aminotransferase gene from *Salvia miltiorrhiza* (Dan-shen) in rosmarinic acid biosynthesis pathway. *Mol. Biol. Rep. 35*, 601−612.

(14) Xiao, Y., Di, P., Chen, J., Liu, Y., Chen, W., and Zhang, L. (2009) Characterization and expression profiling of 4-hydroxyphenylpyruvate dioxygenase gene (Smhppd) from *Salvia miltiorrhiza* hairy root cultures. *Mol. Biol. Rep. 36*, 2019−2029.

(15) Zhao, S., Hu, Z., Liu, D., and Leung, F. C. C. (2006) Two divergent members of 4-coumarate: Coenzyme A ligase from *Salvia miltiorrhiza* Bunge: cDNA cloning and functional study. *J. Integr. Plant Biol. 48*, 1355−1364.

(16) Sander, M., and Petersen, M. (2011) Distinct substrate specificities and unusual substrate flexibilities of two hydroxycinnamoyltransferases, rosmarinic acid synthase and hydroxycinnamoyl-CoA:shikimate hydroxycinnamoyl-transferase, from *Coleus blumei* Benth. *Planta 233*, 1157−1171.

(17) Chen, H., Chen, F., Zhang, Y., and Song, J. (1999) Production of rosmarinic acid and lithospermic acid B in Ti transformed *Salvia miltiorrhiza* cell suspension cultures. *Process Biochem. 34*, 777−784.

(18) Xiao, Y., Gao, S., Di, P., Chen, J., Chen, W., and Zhang, L. (2010) Lithospermic acid B is more responsive to silver ions (Ag+) than rosmarinic acid in *Salvia miltiorrhiza* hairy root cultures. *Biosci. Rep. 30*, 33−40.

(19) Xiao, Y., Gao, S., Di, P., Chen, J., Chen, W., and Zhang, L. (2009) Methyl jasmonate dramatically enhances the accumulation of phenolic acids in *Salvia miltiorrhiza* hairy root cultures. *Physiol. Plant. 137*, 1−9.

(20) Szewczuk, L. M., Lee, S. H., Blair, I. A., and Penning, T. M. (2005) Viniferin formation by COX-1: evidence for radical intermediates during co-oxidation of resveratrol. *J. Nat. Prod. 68*, 36−42.

(21) Ponzoni, C., Beneventi, E., Cramarossa, M. R., Raimondi, S., Trevisi, G., Pagnoni, U. M., Riva, S., and Forti, L. (2007) Laccase-catalyzed dimerization of hydroxystilbenes. *Adv. Synth. Catal. 349*, 1497−1506.

(22) Shang, Y., Qian, Y., Liu, X., Dai, F., Shang, X., Jia, W., Liu, Q., Fang, J., and Zhou, B. (2009) Radical-scavenging activity and mechanism of resveratrol-oriented analogues: influence of the solvent, radical, and substitution. *J. Org. Chem. 74*, 5025−5031.

(23) D'Auria, J. C (2006) Acyltransferases in plants: a good time to be BAHD. *Curr. Opin. Plant Biol. 9*, 331−340.

(24) Berger, A., Meinhard, J., and Petersen, M. (2006) Rosmarinic acid synthase is a new member of the superfamily of BAHD acyltransferases. *Planta 224*, 1503−1510.

(25) Landmann, C., Hücherig, S., Fink, B., Hoffmann, T., Dittlein, D., Coiner, H. A., Schwab, W., Thomas, F., and Hu, S. (2011) Substrate promiscuity of a rosmarinic acid synthase from lavender (*Lavandula angustifolia* L.). *Planta 234*, 305−320.

(26) Yu, X., Gou, J., and Liu, C. (2009) BAHD superfamily of acyl-CoA dependent acyltransferases in *Populus* and *Arabidopsis*: bioinformatics and gene expression. *Plant Mol. Biol. 70*, 421−442.

(27) Yu, X., Chen, M., and Liu, C. (2008) Nucleocytoplasmic-localized acyltransferases catalyze the malonylation of 7- O- glycosidic (iso)flavones in *Medicago truncatula*. *Plant J. 55*, 382−396.

(28) Gang, D. R., Beuerle, T., Ullmann, P., Werck-Reichhart, D., and Pichersky, E. (2002) Differential production of meta hydroxylated phenylpropanoids in sweet basil peltate glandular trichomes and leaves is controlled by the activities of specific acyltransferases and hydroxylases. *Plant Physiol. 130*, 1536−1544.

(29) Schuler, M. A. (1996) Plant Cytochrome P450 Monooxygenases. *Crit. Rev. Plant Sci. 15*, 235−284.

(30) Werck-Reichhart, D., Bak, S., and Paquette, S. (2002) Cytochromes P450, in *The Arabidopsis Book*, e0028, The American Society of Plant Biologists, Rockville, MD.

(31) Mizutani, M., Ohta, D., and Sato, R. (1997) Isolation of a cDNA and a genomic clone encoding cinnamate 4-hydroxylase from Arabidopsis and its expression manner in planta. *Plant Physiol. 113*, 755−763.

(32) Bassard, J. E., Richert, L., Geerinck, J., Renault, H., Duval, F., Ullmann, P., Schmitt, M., Meyer, E., Mutterer, J., Boerjan, W., De Jaeger, G., Mely, Y., Goossens, A., and Werck-Reichhart, D. (2012) Protein-protein and protein-membrane associations in the lignin pathway. *Plant Cell 24*, 4465−4482.

(33) Bayburt, T. H., and Sligar, S. G. (2002) Single-molecule height measurements on microsomal cytochrome P450 in nanometer-scale phospholipid bilayer disks. *Proc. Natl. Acad. Sci. U.S.A. 99*, 6725−6730.

(34) Matsuno, M., Nagatsu, A., Ogihara, Y., Ellis, B. E., and Mizukami, H. (2002) CYP98A6 from *Lithospermum erythrorhizon* encodes 4-coumaroyl-4′-hydroxyphenyllactic acid 3-hydroxylase involved in rosmarinic acid biosynthesis. *FEBS Lett. 514*, 219−224.

(35) Schoch, G., Goepfert, S., Morant, M., Hehn, A., Meyer, D., Ullmann, P., and Werck-Reichhart, D. (2001) CYP98A3 from *Arabidopsis thaliana* is a 3′-hydroxylase of phenolic esters, a missing link in the phenylpropanoid pathway. *J. Biol. Chem. 276*, 36566−36574.

(36) Zheng, Z., Qualley, A., Fan, B., Dudareva, N., and Chen, Z. (2009) An important role of a BAHD acyl transferase-like protein in plant innate immunity. *Plant J. Cell Mol. Biol. 57*, 1040−1053.

(37) Pezet, R. (1998) Purification and characterization of a 32-kDa laccase-like stilbene oxidase produced by Botrytis cinerea Pers .: Fr. *FEMS Microbiol. Lett. 167*, 203−208.
(38) Giardina, P., Faraco, V., Pezzella, C., Piscitelli, A., Vanhulle, S., and Sannia, G. (2010) Laccases: a never-ending story. *Cell. Mol. Life Sci. 67*, 369−385.